

High-intensity laser-accelerated ion beam produced from cryogenic micro-jet target

M. Gauthier, J. B. Kim, C. B. Curry, B. Aurand, E. J. Gamboa, S. Göde, C. Goyon, A. Hazi, S. Kerr, A. Pak, A. Propp, B. Ramakrishna, J. Ruby, O. Willi, G. J. Williams, C. Rödel, and S. H. Glenzer

Citation: *Review of Scientific Instruments* **87**, 11D827 (2016); doi: 10.1063/1.4961270

View online: <http://dx.doi.org/10.1063/1.4961270>

View Table of Contents: <http://scitation.aip.org/content/aip/journal/rsi/87/11?ver=pdfcov>

Published by the [AIP Publishing](#)

Articles you may be interested in

[Investigation of relativistic intensity laser generated hot electron dynamics via copper K \$\alpha\$ imaging and proton acceleration](#)

Phys. Plasmas **20**, 123112 (2013); 10.1063/1.4853575

[Influence of target system on the charge state, number, and spectral shape of ion beams accelerated by femtosecond high-intensity laser pulses](#)

Phys. Plasmas **14**, 033101 (2007); 10.1063/1.2695277

[Quasi-mono-energetic ion acceleration from a homogeneous composite target by an intense laser pulse](#)

Phys. Plasmas **13**, 122705 (2006); 10.1063/1.2404928

[Reduction of proton acceleration in high-intensity laser interaction with solid two-layer targets](#)

Phys. Plasmas **13**, 123101 (2006); 10.1063/1.2395928

[Plasma jets produced in a single laser beam interaction with a planar target](#)

Phys. Plasmas **13**, 062701 (2006); 10.1063/1.2206171



High-intensity laser-accelerated ion beam produced from cryogenic micro-jet target

M. Gauthier,^{1,a)} J. B. Kim,¹ C. B. Curry,¹ B. Aurand,² E. J. Gamboa,¹ S. Göde,¹ C. Goyon,³ A. Hazi,³ S. Kerr,⁴ A. Pak,³ A. Propp,¹ B. Ramakrishna,⁵ J. Ruby,³ O. Willi,² G. J. Williams,³ C. Rödel,^{1,6} and S. H. Glenzer¹

¹SLAC National Accelerator Laboratory, Menlo Park, California 94025, USA

²Heinrich-Heine-University Düsseldorf, Düsseldorf, Germany

³Lawrence Livermore National Laboratory, Livermore, California 94551, USA

⁴University of Alberta, Edmonton, Alberta T6G 1R1, Canada

⁵Indian Institute of Technology, Hyderabad, India

⁶Friedrich-Schiller-University Jena, Jena, Germany

(Presented 7 June 2016; received 10 June 2016; accepted 26 July 2016; published online 24 August 2016)

We report on the successful operation of a newly developed cryogenic jet target at high intensity laser-irradiation. Using the frequency-doubled Titan short pulse laser system at Jupiter Laser Facility, Lawrence Livermore National Laboratory, we demonstrate the generation of a pure proton beam with maximum energy of 2 MeV. Furthermore, we record a quasi-monoenergetic peak at 1.1 MeV in the proton spectrum emitted in the laser forward direction suggesting an alternative acceleration mechanism. Using a solid-density mixed hydrogen-deuterium target, we are also able to produce pure proton-deuteron ion beams. With its high purity, limited size, near-critical density, and high-repetition rate capability, this target is promising for future applications. *Published by AIP Publishing.* [<http://dx.doi.org/10.1063/1.4961270>]

I. INTRODUCTION

Ion beams accelerated with high-intensity lasers through the target normal sheath acceleration (TNSA) mechanism show exceptional properties such as high brightness, high spectral cut-off, high directionality, low emittance, and short duration (a few ps at the source).¹ These characteristics have already been used successfully in fundamental research experiments to generate warm dense matter (WDM),² or for proton radiography.³ Many other interesting applications have been suggested for use in medicine,⁴ nuclear physics,⁵ accelerators,⁶ astrophysics,⁷ and in inertial confinement fusion (ICF) experiments.⁸ Nevertheless, most of the requirements for applications in terms of ion energy, conversion efficiency, spectral width, brilliance, and suitability for high-repetition rate operations have not been achieved yet. To overcome the limitations of TNSA, recent studies using particle-in-cell (PIC) simulations have shown that using higher laser intensities and tailored high-density targets can access favorable regimes of laser ion acceleration.⁹⁻¹¹

In this paper, we report a study of ions accelerated using a recently developed cryogenic hydrogen microjet source to work towards a proton source with enhanced emittance, flux, and energy. In addition, owing to its stability and compatibility to high-repetition rates,¹² this unique target has the potential to address many of the ion source requirements mentioned above. We describe the experimental platform and present the first

measurements of ions produced from a cryogenic hydrogen jet using high-intensity laser irradiation. After characterizing the typical ion beam spectrum accelerated by the Titan short pulse laser at Jupiter Laser Facility, Lawrence Livermore National Laboratory, we discuss the advantages of this advanced target for alternative enhanced ion acceleration mechanisms.

II. EXPERIMENTAL PLATFORM

The cryogenic hydrogen jet consists on a continuous flow helium cryostat. Cooled down to a temperature of ~ 17 K, the liquid hydrogen emerges from a thin $10\ \mu\text{m}$ diameter orifice with a flow of around 100-200 sccm (see Figs. 1(a) and 1(b)). The liquid hydrogen jet cools by evaporation and freezes with minimal mass loss, producing a continuous $10\ \mu\text{m}$ diameter cylinder of solid-density hydrogen (0.07-0.08 g/cc) as shown in Fig. 1(c). The liquid hydrogen solidifies within the first few hundred microns depending on the hydrogen flow, temperature, and aperture size. The hydrogen target propagates into vacuum at a velocity of ~ 50 -100 m/s, thus minimizing the mass loss due to sublimation at the laser interaction point typically located < 20 mm away from the nozzle.¹³

Ultra-high intensity laser pulses are typically focused to a few to $10\ \mu\text{m}$ focal spot diameter (full width at half-maximum (FWHM)) on a Rayleigh length of a few tens to $100\ \mu\text{m}$. The limited size of the hydrogen target in two dimensions makes stability and precision of alignment mandatory, especially for a low-shot rate laser system such as Titan. Two high-magnification, long working distance objectives, well-separated in angle ($> 60^\circ$) are therefore used to determine the target position. Two actuators attached to the breadboard

Note: Contributed paper, published as part of the Proceedings of the 21st Topical Conference on High-Temperature Plasma Diagnostics, Madison, Wisconsin, USA, June 2016.

^{a)}maxence.gauthier@stanford.edu

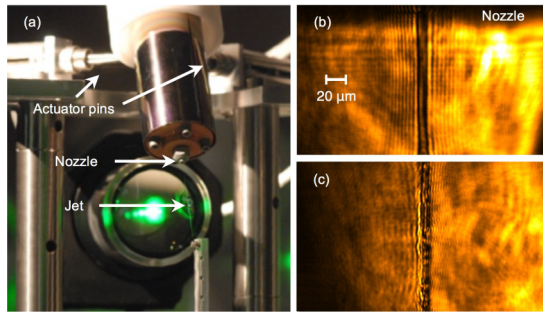


FIG. 1. (a) The nozzle of the cryogenic hydrogen jet is stabilized and positioned precisely by two actuator pins. (b) High magnification imaging of the $10\ \mu\text{m}$ diameter cryogenic hydrogen jet, respectively, in a liquid state at the output of the nozzle and (c) in a solid state 10 mm below the nozzle.

(see Fig. 1(a)) damp any vibrations coming from the vacuum chamber on which the jet is attached to, and align the jet with micrometer precision. Using this method, the spatial jitter of the jet measured 20 mm from the nozzle is typically $\pm 4\ \mu\text{m}$, comparable to the transverse laser focal spot jitter.

Another important aspect in the operation of the hydrogen source is the downtime required for the cooling and warm up procedure of the source, 3–4 h in total. Therefore, diagnostics compatible with limited-to-no access of the inside of the target chamber between shots are recommended. Nevertheless, with its compact size and $< 5 \times 10^{-5}$ mbar vacuum requirement, the micro-jet source is highly appropriate for implementation and use in high-intensity laser facilities such as the ones dedicated to external users where user access is limited.

III. EXPERIMENTAL SET-UP

A schematic of the experimental setup is shown in Fig. 2. The Titan laser is frequency doubled to enhance the pulse intensity contrast:¹⁴ owing to its high energy (~ 140 J at 1057 nm) and comparably long duration (700 fs), the laser pulse is indeed prone to produce a pre-pulse that would significantly expand the target before the main irradiation, thus degrading ion acceleration. This effect is even more critical in our case due to the limited target size, moderate density, and low-Z, resulting in a high expansion velocity. A f/3 off-axis parabola (OAP) focuses the laser to a 10–13 μm diameter (FWHM) focal spot after optimization with the deformable mirror, and delivers a peak intensity on target estimated at $3\text{--}5 \times 10^{19}$ W/cm². In contrast with protons produced by TNSA accelerated in the target surface normal direction, most of

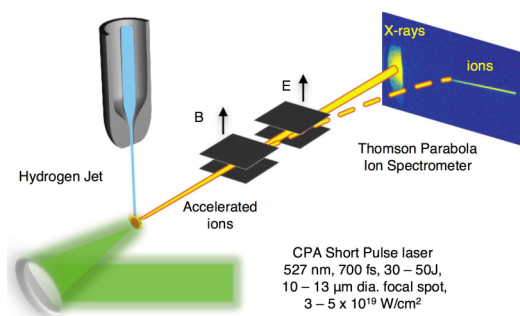


FIG. 2. Experimental setup and laser parameter on target.

the advanced ion acceleration mechanisms^{9–11} are based on enhanced laser coupling efficiency and thus predict an ion emission preferentially in the laser forward direction. In order to differentiate protons generated through these two mechanisms, the laser propagation axis makes an angle of 30° with respect to the target cylindrical axis (TNSA ions are typically emitted in a 20° half-cone angle). A Thomson parabola (TP) records the ions emitted in the direction normal to the target surface, while another one measures the ion spectra produced in the laser forward direction. Each ion beam is collected by a $500\ \mu\text{m}$ diameter pinhole located 1 m away from the interaction. After being deflected by a 1.1 T magnetic field to differentiate ions of different velocity and by a 4.0 kV/cm electric field to differentiate ions of different charge-to-mass ratio, the ions deposit their energy on a FujiFilm BAS-TR image plate (IP) detector. In order to avoid noise and high voltage arcing, a differential pumping system is implemented between the TP and the target chamber to ensure a pressure below 10^{-5} mbar.

IV. RESULTS AND DISCUSSION

On the IP raw images shown in Fig. 3(a) only the line corresponding to protons is visible. In comparison with regular planar foils shown in Fig. 3(c), the cryogenic target surface does not show any heavier ions from hydrocarbon contaminants (e.g. carbon, oxygen) when irradiated. In this high-intensity interaction, only the ions present initially in the

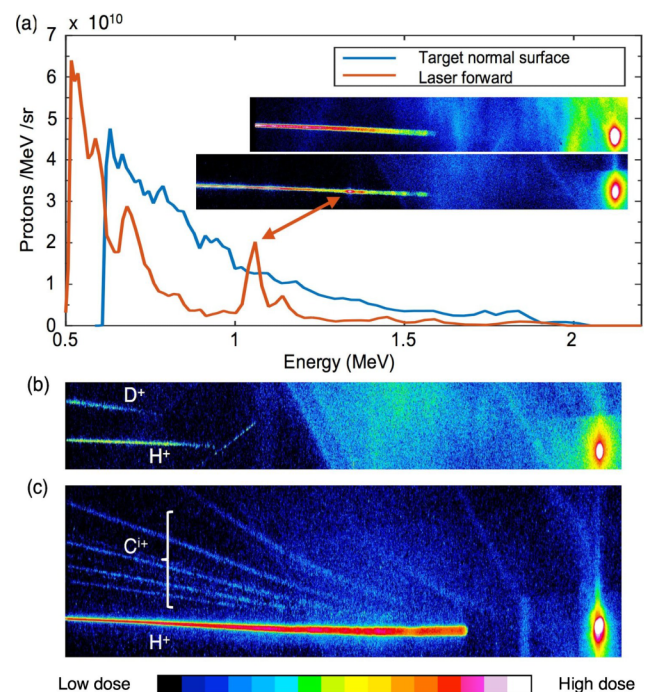


FIG. 3. (a) Raw images of IPs recorded in the target normal and laser forward direction during a high-intensity shot on hydrogen. The corresponding proton spectra are computed using an absolute calibration of the signal on the IP;¹⁸ raw IP image from the laser forward TP obtained when irradiating, (b) the cryogenic source fed by a mixture of H_2 and D_2 gas (3:1), (c) a $7\ \mu\text{m}$ thick planar aluminum foil. The color scaling used for IP images is logarithmic with respect to the ion dose and is adjusted to improve the contrast.

target, in this case protons, are accelerated. This degree of ion beam purity produced by TNSA has never been achieved using other target designs or preparation methods. Future nuclear and medical applications^{5,15} have interest in preferential acceleration of heavier ions such as deuterons or carbon. Similar results can be achieved when using any pure gas compatible with the cryogenic source.¹³ For instance, a pure deuteron beam has been produced at SLAC National Accelerator Laboratory from a pure deuterium cryogenic target.¹⁶ We notice that maximum proton energy and flux are relatively low compared to what can be obtained using standard metallic foils under identical laser conditions. Using $7\ \mu\text{m}$ Al foil, the same laser system typically accelerates an order of magnitude more protons to the 1 MeV energies and produces proton beams with energy cut-off up to 8 MeV (see Fig. 3(c)). This difference can be explained by two main reasons: (i) the focal spot diameter is comparable if not larger than the target, so a non-negligible portion of the beam is not interacting with the target; (ii) the target cylindrical geometry induces TNSA ions to be emitted at 360° instead of 40° , which inherently reduces the ion flux measured within a given solid angle. Work is currently underway to develop new rectangular shaped apertures that would allow us to produce wider and thinner planar targets.

When comparing the two spectra in Fig. 3(a), one notes that protons are present in higher number in the target surface normal direction and exhibit a semi-Maxwellian spectrum typical of TNSA. The laser forward spectrum is significantly modulated in the high energy part showing a strong proton quasi-monoenergetic peak at 1.1 MeV, with an energy spread of 4% (FWHM). This suggests that an acceleration mechanism different from the standard TNSA occurs in the laser forward direction. Secondly, the absence of modulations in the ion spectrum produced from an aluminum planar of comparable thickness (Fig. 3(c)) indicates the importance of the target density on the onset of this mechanism. Although further analysis and simulations are required to determine which acceleration regime is responsible for the modulations, these preliminary results are very encouraging for applications. For instance, the monoenergetic feature shows already sufficient ion energy and flux for ion probing in stopping power measurements of WDM.¹⁷

Cryogenic micro-jet targets are highly appropriate to study alternative acceleration processes. First, laser conversion efficiency is predicted to be the most efficient when the target gets closer to relativistic critical density. For a cryogenic hydrogen target, this regime is already achievable with some of the currently available PW laser systems, e.g., $\sim 10^{21}\ \text{W}/\text{cm}^2$ for 527 nm laser light. In addition, direct comparison with 2D and 3D PIC simulations is possible due to the low-Z and moderate density of the target. To investigate the effect of chemically mixed target and ion charge-to-mass ratio on ion

acceleration processes, we are also able to produce a solid-density mixed hydrogen/deuterium target by using a mixed gas of H_2 and D_2 for input of the cryogenic source. The proportion of each species is chosen by applying different pressures for each gas input. To illustrate this capability, we show in Fig. 3(b) the TP traces obtained after irradiation of a (3:1) hydrogen/deuterium target. The two ion traces visible on the IP indicate the production of a pure broadband proton and deuteron beam. Unfortunately the laser energy was low during this shot, thus no meaningful comparison can be performed with the pure hydrogen case.

V. CONCLUSION

Using a cryogenic hydrogen microjet target, we demonstrated that a multi-MeV pure proton beam can be produced through high-intensity laser interaction. The high purity, limited size, moderate density, and mixed target capabilities make this target highly favorable for study and realization of enhanced ion acceleration mechanisms, as illustrated by the 1.1 MeV quasi-monoenergetic proton peak recorded in the laser forward direction. Future experiments will aim to improve ion beam production by testing asymmetric jets at higher laser intensities and repetition rates.

ACKNOWLEDGMENTS

We thank the Jupiter Laser Facility crew for their excellent user support. This work was supported by the U.S. DOE Office of Science, Fusion Energy Science under FWP No. 100182, by SLAC Laboratory Directed Research and Development, and by LLNL under Contract No. DE-AC52-07NA27344 and the U.S. DOE Office of Science, Fusion Energy Science ACE HEDLP Diagnostics. C.R. acknowledges funding from the Volkswagen Foundation.

¹J. Fuchs *et al.*, *Nat. Phys.* **2**, 48–54 (2006).

²P. K. Patel *et al.*, *Phys. Rev. Lett.* **91**, 125004 (2004).

³L. Romagnani *et al.*, *Phys. Rev. Lett.* **95**, 195001 (2005).

⁴J. Weichsel, T. Fuchs *et al.*, *Phys. Med. Biol.* **53**, 4383 (2008).

⁵A. G. Krygier *et al.*, *Phys. Plasmas* **22**, 053102 (2015).

⁶T. E. Cowan *et al.*, *Phys. Rev. Lett.* **92**, 204801 (2004).

⁷B. A. Remington, D. Arnett *et al.*, *Science* **284**, 1488 (1999).

⁸M. Roth *et al.*, *Phys. Rev. Lett.* **86**, 436 (2001).

⁹A. P. L. Robinson *et al.*, *New J. Phys.* **10**, 013021 (2008).

¹⁰L. Yin, B. J. Albright *et al.*, *Phys. Rev. Lett.* **107**, 045003 (2011).

¹¹D. Haberberger, S. Tochitsky *et al.*, *Nat. Phys.* **8**, 95 (2012).

¹²U. Zastra *et al.*, *Phys. Rev. Lett.* **112**, 105002 (2014); S. H. Glenzer *et al.*, *J. Phys. B: At., Mol. Opt. Phys.* **49**, 092001 (2016).

¹³J. B. Kim *et al.*, *Rev. Sci. Instrum.* **87**, 11E328 (2016).

¹⁴D. Neely *et al.*, *Laser Part. Beams* **18**, 405–409 (2000).

¹⁵B. M. Hegelich *et al.*, *Nature* **439**, 441–444 (2006).

¹⁶M. Gauthier *et al.*, SLAC Technical Report No. 1061, 2016.

¹⁷M. Gauthier *et al.*, *High Energy Density Phys.* **9**, 488–495 (2013).

¹⁸A. Mancic, J. Fuchs *et al.*, *Rev. Sci. Instrum.* **79**, 073301 (2008).